JOURNAL OF PHYSICAL ORGANIC CHEMISTRY
J. Phys. Org. Chem. 2001; **14:** 481–487
DOI:10.1002/poc.393

Computer-aided design of selective COX-2 inhibitors: comparative molecular field analysis and docking studies of some 3,4-diaryloxazolone derivatives

G. R. Desiraju,[1]* J. A. R. P. Sarma,[2]* D. Raveendra,[2] B. Gopalakrishnan,[3]* R. Thilagavathi,[3] M. E. Sobhia[3] and H. S. Subramanya[4]

[1]School of Chemistry, University of Hyderabad, Hyderabad 500 046, India
[2]Molecular Modelling Group, Organic Division-I, Indian Institute of Chemical Technology, Hyderabad 500 007, India
[3]Department of Medicinal Chemistry, National Institute of Pharmaceutical Education and Research, S. A. S. Nagar 160 062, India
[4]Membrane Biology Division, Central Drug Research Institute, Lucknow, 226 001, India

Received 21 December 2000; Revised 10 April 2001; Accepted 12 April 2001

ABSTRACT: The recent discovery of a second, inducible isoform of cyclooxygenase, COX-2, has stimulated the search for highly selective non-steroidal anti-inflammatory drugs (NSAIDs). These NSAIDs have the ability to treat pain and inflammation caused by arthritis with less risk of gastrointestinal or renal toxicity. We report here the results of 3D-quantitative structure–activity relationship and docking studies, performed on a series of 3,4-diaryloxazolones. Comparative moleculer field analysis studies provided a good model with cross-validated and conventional r^2 values of 0.688 and 0.969 respectively for 24 analogues in the training set with six components. Docking studies with both COX-1 and COX-2 indicate good selectivity for COX-2. The binding energies between COX-2 and some of the most active oxazolones are comparable to those of celecoxib or rofecoxib. These compounds adopt similar orientations and form similar sets of hydrogen bonds involving the sulfonyl group of the ligand and His 90, Leu 352, Ser 353, Arg 513, Phe 518 and Ser 530 residues of the receptor. Copyright © 2001 John Wiley & Sons, Ltd.

KEYWORDS: selective COX-2 inhibitors; diaryloxazolones; CoMFA; docking studies

INTRODUCTION

The quest for selective COX-2 inhibitors began when this enzyme was first described in 1990.[1–6] It is now well established that cyclooxygenase exists in at least two isoforms: COX-1 and COX-2. COX-1 is a regulatory enzyme that is present almost throughout the body and produces prostaglandins that help in proper kidney and stomach functioning. COX-2 is an inducible enzyme that catalyzes the production of prostaglandins leading to inflammation.[7,8] Most of the existing non-steroidal anti-inflammatory drugs (NSAIDs) suffer from non-selective binding to both COX-1 and COX-2, thus producing undesirable gastrointestinal and renal side effects. It is believed that inhibitors that bind with a greater or lesser extent of selectivity towards COX-2 are different from the traditional anti-inflammatory drugs. Furthermore, selective COX-2 inhibitors are believed to play a vital role in ovulation and labour, as well as in the treatment of colon cancer and Alzheimer's disease.[7,9–11]

Different research groups have developed many novel COX-2 inhibitors in the past few years.[12–16] Meloxicam, which has 100-fold specificity towards COX-2 over COX-1, is widely used for the treatment of rheumatoid arthritis.[7,17] Nimesulide, which has been classified as a preferential COX-2 inhibitor with 10–50-fold potency, has been in clinical usage for the past 6 years[7,8]. Similarly, Etodolac is a COX-2 inhibitor, which is marketed in Europe and North America for the treatment of osteoarthritis.[7,18] Recently, highly potent diaryl heterocyclic compounds have been identified as selective COX-2 inhibitors; notably, two of them, celecoxib (**I**) and rofecoxib (**II**) have been approved by the Food and Drug Administration, USA. These drugs have shown efficacy in the clinical trials of acute pain, osteoarthritis and rheumatoid arthritis.[19,20] SC-558 (**III**), which is an another diaryl heterocyclic inhibitor, has ~1900-fold selectivity for COX-2 over COX-1.[21] Valdecoxib is another diaryl heterocyclic inhibitor currently in clinical evaluation for the treatment of pain and inflammation.[22] Different analogues of rofecoxib have recently been

**Correspondence to:* G. R. Desiraju, School of Chemistry, University of Hyderabad, Hyderabad 500 046, India; J. A. R. P. Sarma, Molecular Modelling Group, Organic Division-1, Indian Institute of Chemical Technology, Hyderabad 500 007, India or B. Gopalakrishnan, Department of Medicinal Chemistry, National Institute of Pharmaceutical Education and Research, S. A. S. Nagar 160 062, India.
Contract/grant sponsor: CSIR; *Contract/grant number:* 90/008/99/EMR-II.

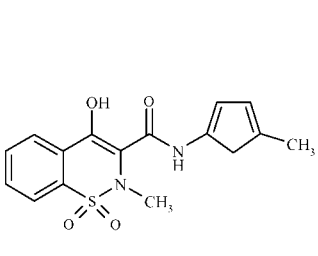

Meloxicam

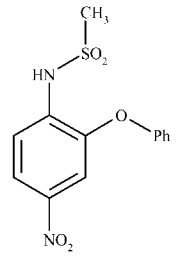

Nimesulide

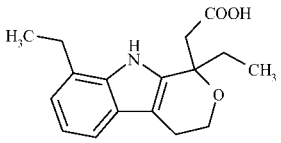

Etodolac

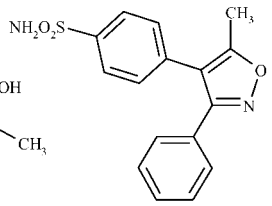

Valdecoxib

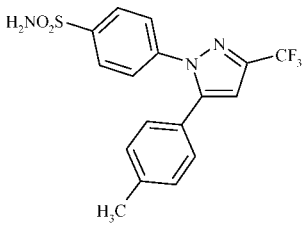

Celecoxib, **I**

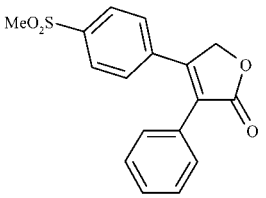

Rofecoxib, **II**

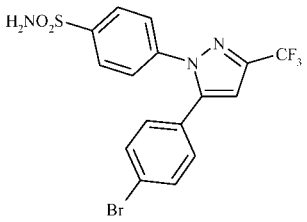

SC-558, **III**

reported to be potent and orally active.[12,20] Analysis of the *q*uantitative *s*tructure–*a*ctivity *r*elationships (QSARs) of some of these diaryl heterocyclic compounds for COX-2 selectivity has been explored by us.[23] Recently, Puig *et al.*[24] have reported a novel series of 3,4-diaryloxazolones that are structurally similar to both **I** and **II**, and are shown to be selective COX-2 inhibitors. In this paper, comparative molecular field analysis (CoMFA) and structure-based docking studies of this series of oxazolone derivatives are reported.

COMPUTATIONAL DETAILS

Molecular modelling and CoMFA studies were carried out using the QSAR module as implemented in SYBYL.[25] A series of 29 3,4-diaryloxazolone analogues were selected for CoMFA; 24 of the molecules were included in the training set and the remaining molecules were treated as the test set. The biological activities were converted into the corresponding pIC_{50} values. All molecules were generated from molecule **III**.[21,26] All structures were minimized using Tripos force fields and the conjugate gradient algorithm with a gradient convergence value of 0.05 kcal mol^{-1} Å^{-1}. Partial atomic charges were calculated using the Gasteiger–Hückel method. Initially, a constrained minimization for 100 cycles was performed in which the three rings, A, B and C (Scheme 1), were defined as an aggregate to constrain their conformation. This procedure was employed in order to prevent the conformation moving to a false region. The constraints were then removed and the structure was subjected to 500 cycles of minimization till the gradient converged to 0.05 kcal mol^{-1} Å^{-1}.

The most active compound **29**, was used as the reference and the rest of the molecules were aligned to it by using fragments 1–3 (Table 1). The molecular alignments were carried out with the SYBYL database alignment method. Molecular alignment has also been carried out with field fit methods, where the steric and electrostatic fields of various molecules were fitted onto the most active molecule's steric and electrostatic fields with minimum deviation. However, the best results with respect to the training set and test set were obtained when fragment 1 was used. The steric and electrostatic CoMFA fields were calculated at each lattice intersection of a

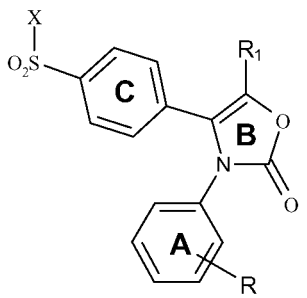

Scheme 1

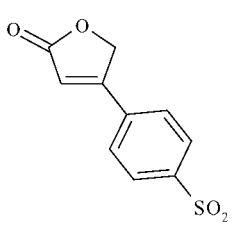

1

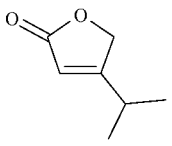

2

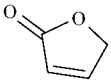

3

Table 1. Summary of CoMFA–PLS results for the training set molecules

Fragment	1	1	1	2	3	4[a]
No. of components	5	**6**	7	6	5	6
r^{2}_{cv} [b]	0.670	**0.688**	0.689	0.497	0.587	0.709
SEP[c]	0.306	**0.307**	0.315	0.389	0.343	0.296
r^{2}[d]	0.963	**0.969**	0.981	0.904	0.922	0.972
SEE[e]	0.102	**0.097**	0.077	0.104	0.149	0.092
F value	94.809	**88.662**	119.945	74.835	42.426	98.805
Steric field contribution	0.732	**0.735**	0.715	0.751	0.690	0.721
Electrostatic field contribution	0.268	**0.265**	0.285	0.244	0.310	0.279
$r^{2}_{\text{Test set}}$	0.483	**0.502**	0.515	0.421	0.311	0.365
$SD_{\text{Test set}}$	0.395	**0.388**	0.389	0.448	0.494	0.449

[a] Alignment is based on the field fit methods.
[b] Cross-validated correlation coefficient.
[c] Standard error of predictions.
[d] Non-cross-validated correlation coefficient.
[e] Standard error of estimate.

regularly spaced grid of 2.0 Å in all three dimensions within the defined region.[27] This was extended beyond the van der Waals envelopes of all molecules by at least 4.0 Å. Both these fields were calculated with the Tripos force field with default options. The CoMFA field energies were truncated at 30 kcal mol^{-1} for both fields. Regression analysis was performed using the partial least squares (PLS) algorithm with the leave-one-out (LOO) method adopted in the cross-validation calculations of QSAR studies. The cross-validation analysis that produced the highest correlation coefficient value with minimum standard error of predictions and with a lower number of components was considered for final non-cross-validated analysis. Even though CoMFA maps were produced for different numbers of components, analysis with six principal components produced good results when fragment 1 was used for alignment. The number of components with respect to other alignments differs, and in each case the best study is given in Table 1. In all cross-validated runs the column filtering was set to 2.0, whereas in non-cross-validated runs this value was set to zero. Equal weights were assigned to the steric and electrostatic descriptors.

Docking studies

Docking studies were carried out using FlexiDock[25] and Affinity[28] modules with the inhibitors celecoxib, rofecoxib and molecules of 3,4-diaryloxazolone series in both forms of cyclooxygenase. The crystal structures of murine apo-cyclooxygenase-II (6COX) with SC-558[21,26] and sheep cyclooxygenase-I (1PGG) with iodoindomethacin (IMM)[29] were used in this study. Water molecules were removed and hydrogen atoms were added to all the residues of the enzymes. Active sites of COX-1 and COX-2 were defined using the inhibitors IMM and SC-558 respectively, and all amino acid residues within a 5.0 Å radius of any of the inhibitor atoms were considered. All docked ligands were prepositioned in an orientation similar to that of IMM or SC-558.

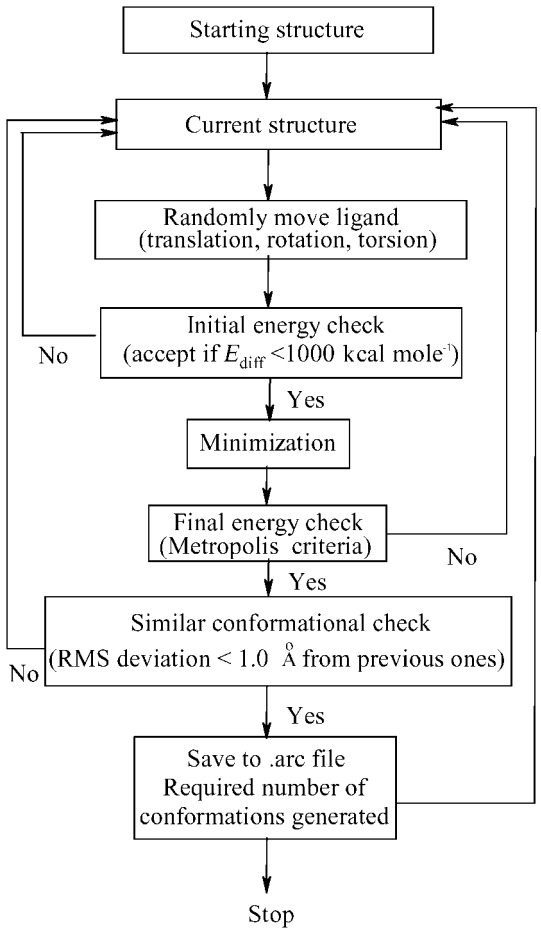

Figure 1. Flowchart of docking procedure adopted by the Affinity module of InsightII. The different criteria adopted for the energy and RMS check are also given

FlexiDock docks a ligand at the predefined location inside the active site of a receptor. Genetic algorithm (GA) methods, which are robust global optimizers and perform well with increasing system size, are employed to determine the ligand geometry inside the active site of the receptor. FlexiDock, which works on a protein–ligand pair, varies the torsional angles of the flexible side chain of the protein, and the ligand can be rotated, and translated with conformational flexibility. The fitness function, which uses a subset of the Tripos force field, namely van der Waals, electrostatic, torsional and constraint energy terms, calculates the energy of the supramolecular system. The docking process starts after the prepositioning of the ligand inside the active site of the receptor with random seed number and user-defined number of generations. A number of docked structural possibilities are generated and sorted on the basis of intermolecular energy.

Tripos force fields with default FlexiDock parameters were used along with Gasteiger charges for both enzymes. Ligand molecules **1–29** generated for the CoMFA studies were used in the docking study. The binding pockets of the enzymes were kept rigid. All rotatable bonds of the ligands were defined to explore the most biologically active conformation. Docking studies were performed for 10^5 generations, and only the energetically favourable structures were analysed. Based on the fitness score (energy), one complex structure for each ligand was selected as the best fit and its score was correlated with its biological activity.

In the Affinity studies, the most active oxazalone **29**, moderately active **18**, less active **25**, celecoxib and rofecoxib ligands were automatically docked (Fig. 1) into the active site of COX-2.[28] In these docking studies, Monte Carlo simulation methods (FixedDocking) were used in order to provide the necessary relaxation to the amino acid residues at the active site, as well as to provide conformational freedom for the ligand. However, the rest of the enzyme was held rigid during the course of the docking search. The extensible systematic force field (ESFF) and its associated charges were used along with Cell—multipole methods to estimate the non-bonded interactions for COX-2. However, previously used geometries with ESFF and Gasteiger–Hückel charges were used for the ligands. The Metropolis criteria of 10 kcal mol^{-1} energy range, 1.0 Å maximum translation and 180° maximum rotation were used for the final energy check. Since the position and orientation of the relatively similar SC-558 is known, all ligands used in this study were believed to bind in a similar way. The aim of using the Metropolis criteria is to find about 30 different orientations that vary very little in energy. However, in some cases, the docking studies have to be terminated, as no further solutions are found even after a prolonged simulation time. Default settings were used for the conformational search of the ligand, as well as in the interaction energy calculations between amino acid residues and the ligands. The dielectric constant was set to 1.0 and no solvation parameters were used. The complex structures obtained during the docking were minimized for 1000 cycles with conjugate gradient methods. Each unique supramolecular structure was further minimized for 3000 cycles or until the gradient converged to a value of 0.01 kcal mol^{-1} $Å^{-1}$ before the interaction energies between various amino acids in the active site were analysed for each ligand.

RESULTS AND DISCUSSION

CoMFA studies

CoMFA with 24 molecules in the training set produced a cross-validated r^2 of 0.688 with minimum standard error and optimum number of components. This analysis was used for the final non-cross-validated run, giving a good correlation coefficient with a very low standard error of estimate (Table 1). The steric and electrostatic contributions are in a 3:1 ratio, indicating the importance of steric fields in the model generation. The actual and calculated inhibitory activities and the residual values for both training and test sets are given in Table 2. The final model demonstrated a good predictive ability by predicting the activities of test set molecules that were not included in the training set.

The final CoMFA gives contour plots of steric and electrostatic interactions. The steric interactions are represented by green- and yellow-coloured contours (Plate 1a). The introduction of bulky substituents in the yellow-coloured region would be expected to lead to decreased biological activity. On the other hand, bulky group substitution in the green-coloured region would increase the activity. Hence, yellow regions around ring A indicate intolerance to bulky substituents. Any large group in the *ortho* position of ring A will force the phenyl ring to adopt a different orientation, resulting in unfavourable interactions between this ring and various amino acid residues of the hydrophobic cleft. A small green-coloured region near the *para* position of ring A shows that medium-sized substituents increase biological activity because of their positioning near the end of the active site cleft that extends towards the peroxide catalytic site. Blue-coloured contours (Plate 1b) represent CoMFA electrostatic fields, and groups with positive potential in these areas (the *meta* or *para* positions of ring A) increase activity.

Molecules **16** and **12** with *ortho* methyl and chloro substituents in ring A are less active. Molecules **4**, **6**, **18**, **20**, **24** and **28** with moderately bulky substituents like chloro, methyl, methoxy in the *para* position are active. However, the bulky ethyl group in **19** reduces the activity; this is also true in molecule **5**, where the combined steric and electronic effects of the trifluoromethyl substituent are decisive. Although the sulfona-

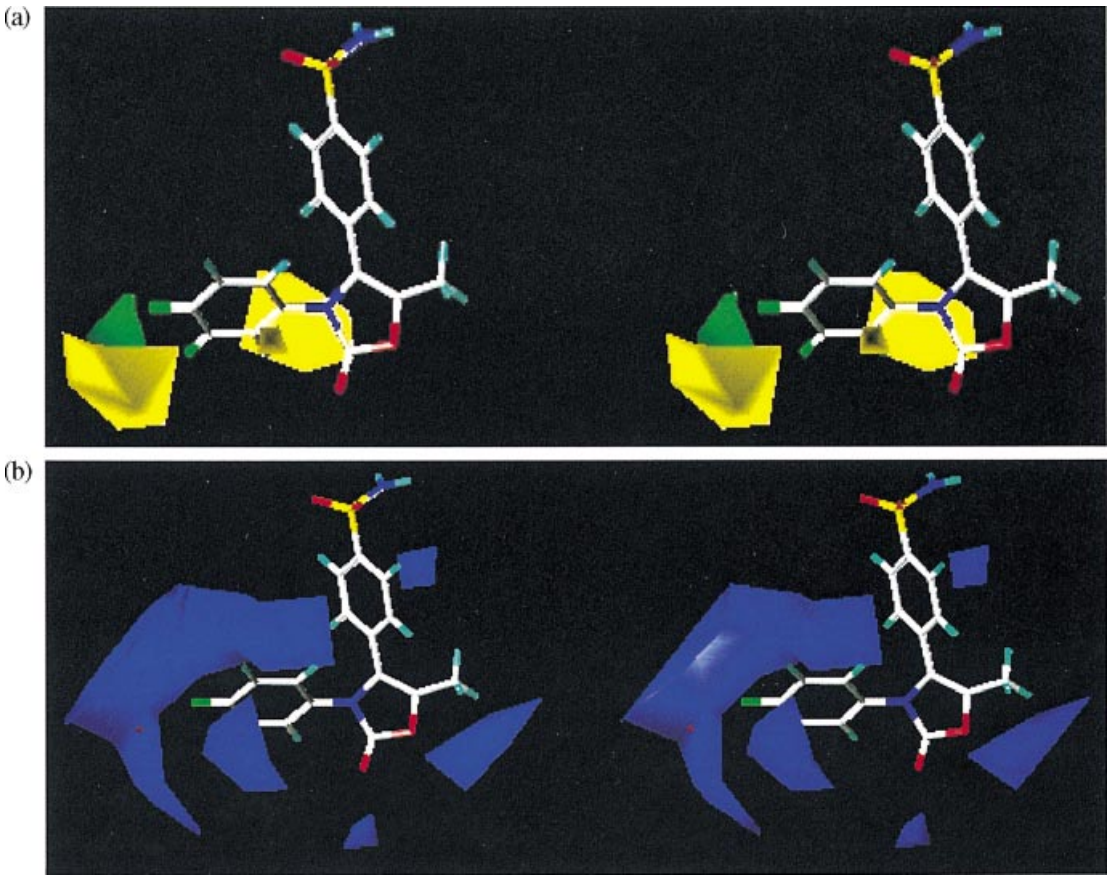

Plate 1. Stereoplots of CoMFA STDEV*COEFF steric (a) and electrostatic (b) fields. Oxazolone molecule **29** is displayed in the background for clarity

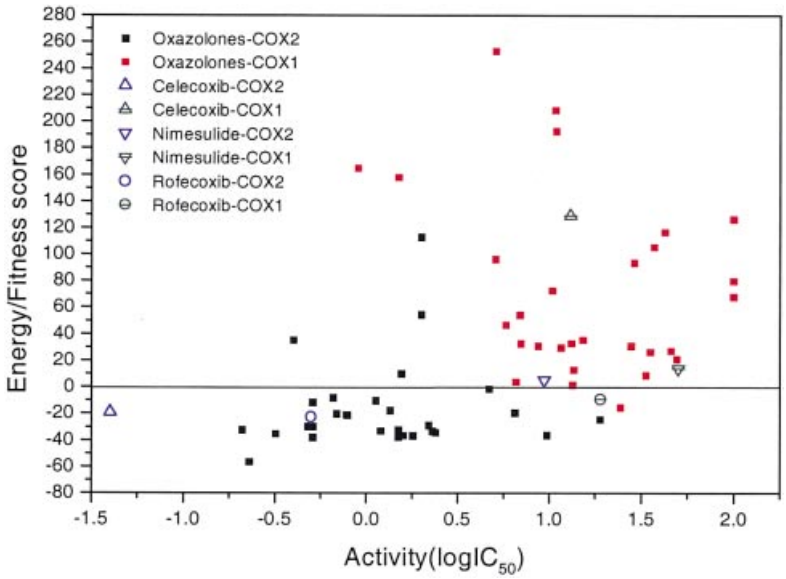

Plate 2. Fitness score versus biological activities of celecoxib, rofecoxib and oxazolones **1**–**29**. The observed biological activities of all ligands with COX-1 and COX-2 are considered as pIC_{50} and are given on the abscissa and the ordinates represent the corresponding scores

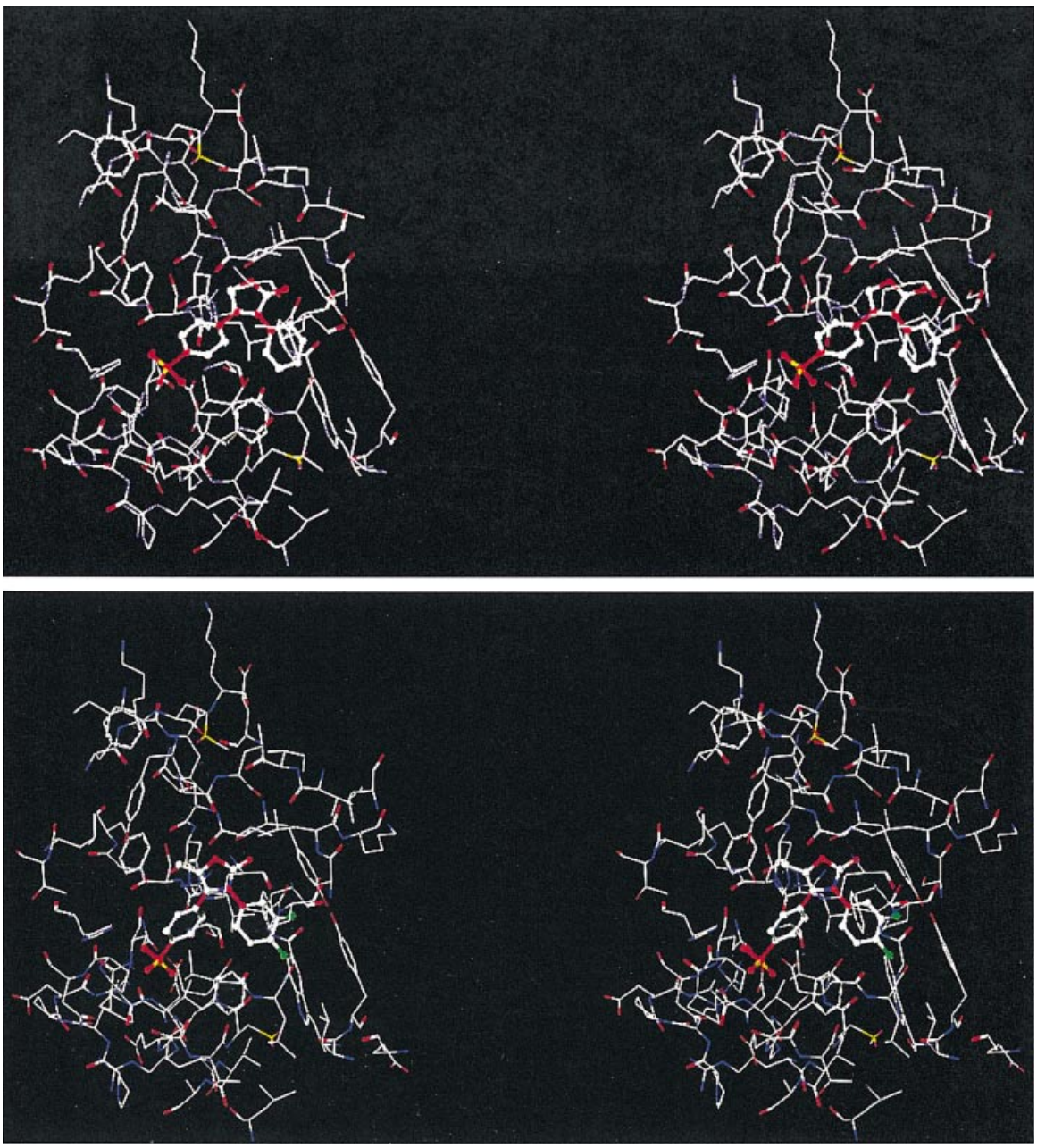

Plate 3. Stereoplots showing the orientation of rofecoxib (a) and oxazolone **29** (b) in the active site of COX-2. The ligands are displayed as ball-and-stick models. All hydrogen atoms were removed for clarity. Note the similar orientation of the two ligands

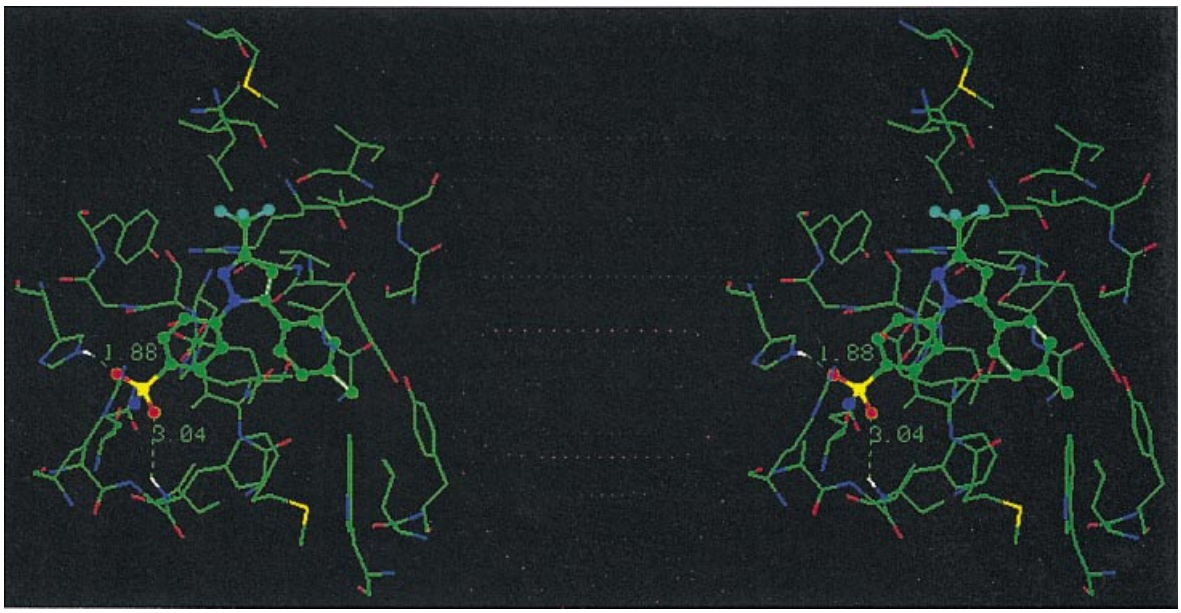

Plate 4. Stereoview of the celecoxib–COX-2 complex. Prominent hydrogen bonds are shown with broken lines

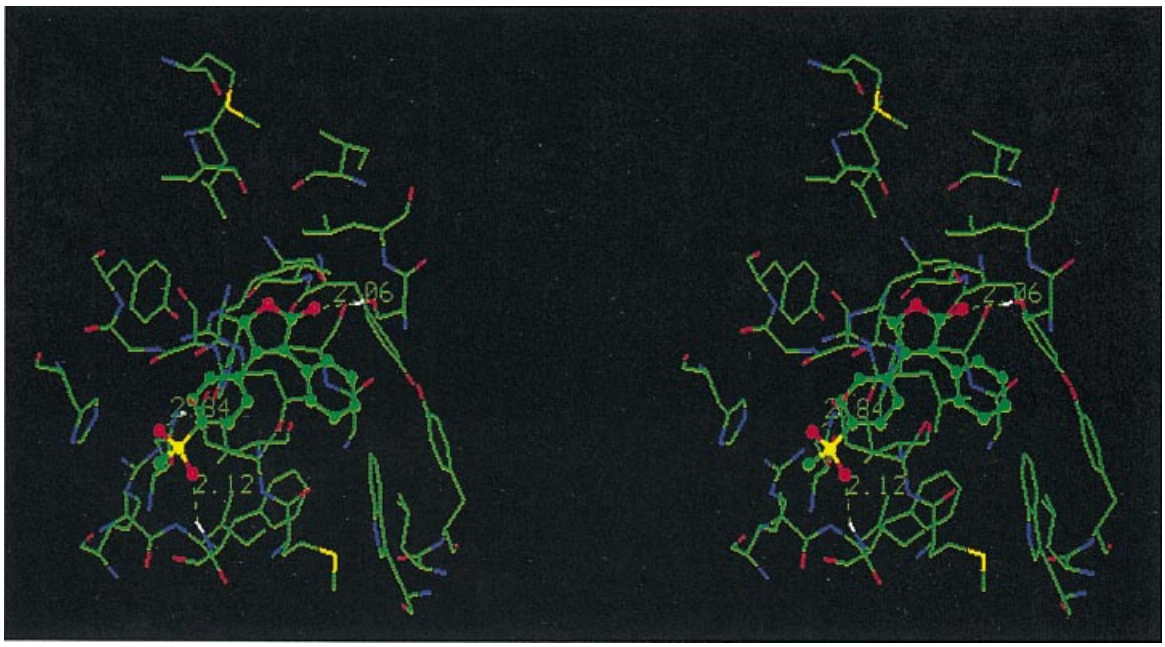

Plate 5. Stereoview of the rofecoxib–COX-2 complex. The hydrogen bonds with Gln 192, Phe 518 and Ser 530 are shown as broken lines

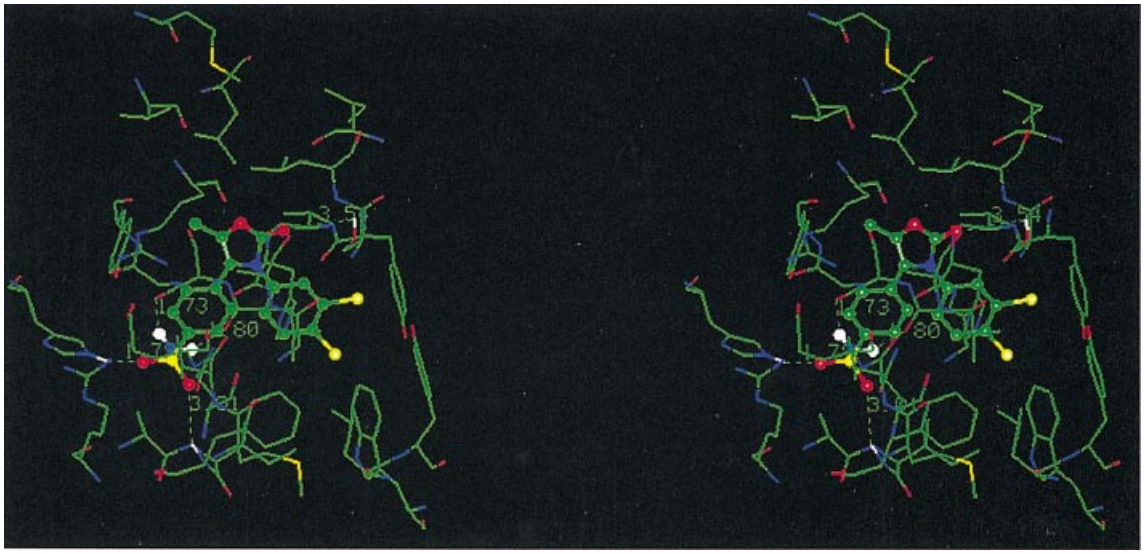

Plate 6. Stereoview of the oxazolone **29**–COX-2 complex. The hydrogen bonds with His 90, Ser 353, Leu 352 and Ser 530 are shown as broken lines

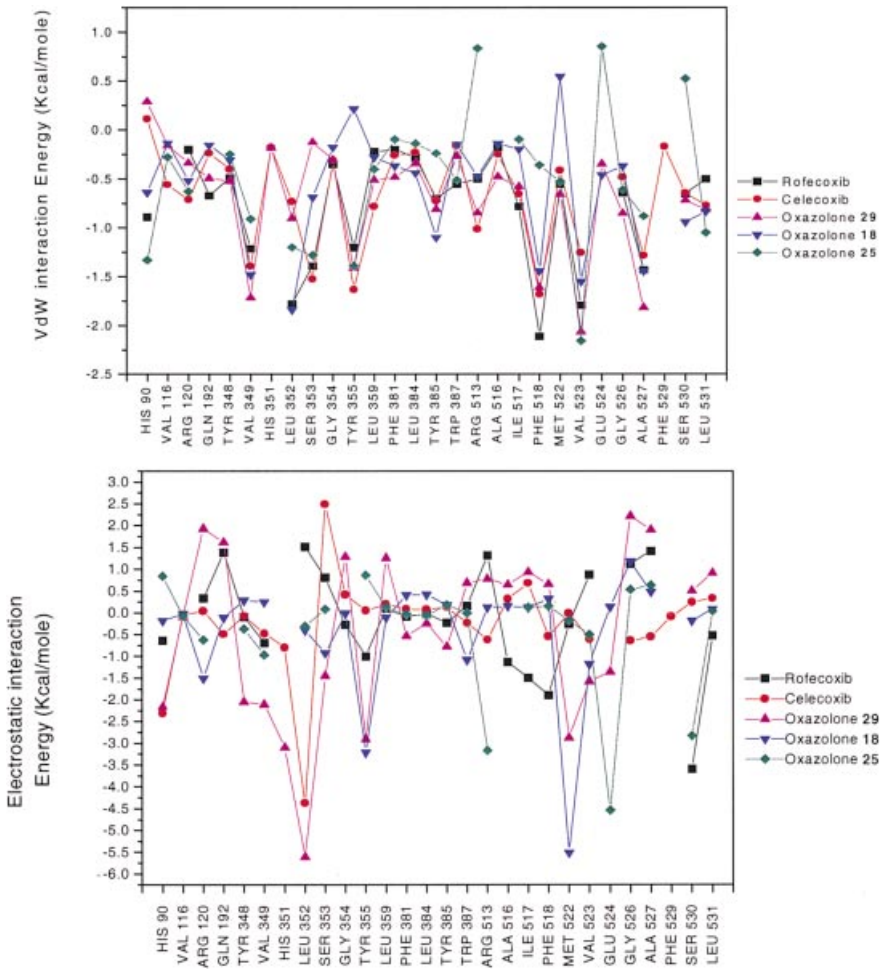

Plate 7. Steric (a) and electrostatic (b) contributions to the non-bonded interaction energies between celecoxib, rofecoxib and oxazolones **29**, **18** and **25** with various residues of the active site of COX-2

Table 2. Experimental and calculated COX-2 inhibitory activities (pIC_{50}) of a number of oxazolone derivatives (Scheme **1**) along with their residuals

Compound	R	X	R_1	Actual	Calculated	Residual
Training set						
1	H	CH_3	H	−0.20	−0.22	0.02
3	4-F	CH_3	H	0.29	0.24	0.05
4	4-Cl	CH_3	H	0.49	0.33	0.16
5	4-CF_3	CH_3	H	−0.30	−0.17	−0.13
6	4-CH_3	CH_3	H	0.32	0.42	−0.10
8	2,4-F_2	CH_3	H	−0.13	−0.12	−0.01
9	H	NH_2	H	−0.38	−0.48	0.10
11	4-F	NH_2	H	−0.18	−0.09	−0.09
12	2-Cl	NH_2	H	−0.81	−0.79	−0.02
13	3-Cl	NH_2	H	−0.18	−0.08	−0.10
14	4-Cl	NH_2	H	−0.08	0.06	−0.14
15	4-CF_3	NH_2	H	−0.30	−0.41	0.11
16	2-CH_3	NH_2	H	−0.99	−1.05	0.06
17	3-CH_3	NH_2	H	0.29	0.24	0.05
18	4-CH_3	NH_2	H	0.10	0.16	−0.06
21	2,4-F_2	NH_2	H	−0.36	−0.36	0.03
22	3,4-Cl_2	NH_2	H	0.40	0.45	−0.05
23	3-F-4-CH_3O	NH_2	H	−0.05	−0.12	0.07
24	3-Cl-4-CH_3O	NH_2	H	0.11	0.12	−0.01
25	Cyclohexyl[a]	NH_2	H	−1.28	−1.25	−0.03
26	1-naphthyl[a]	NH_2	H	−0.67	−0.66	−0.01
27	H	NH_2	CH_3	−0.26	−0.18	−0.08
28	4-F	NH_2	CH_3	0.29	0.23	0.06
29	3,4-Cl_2	NH_2	CH_3	0.64	0.52	0.12
Test set						
2	2-F	CH_3	H	0.18	−0.41	0.59
7	4-C_2H_5	CH_3	H	0.16	0.24	−0.08
10	2-F	NH_2	H	−0.34	−0.68	0.34
19	4-C_2H_5	NH_2	H	−0.19	−0.01	−0.18
20	4-CH_3O	NH_2	H	0.68	0.02	0.66

[a] Cyclohexyl and naphthyl groups replace the respective phenyl groups in **25** and **26**.

mide group is replaced by a sulfomethyl group at the 4′-position of ring C in **1, 3, 4, 5, 6** and **8**, orientational differences are not observed, and the CoMFA fields also do not differ so much as to contribute significantly to the appearance of the contours. This subtle variation in the substituent is one of the important differences between celecoxib and rofecoxib, but is not well-revealed in the CoMFA results. Therefore, we decided to carry out docking studies. Because the oxazolones in this study are similar to both the above drugs, it was felt that such docking studies would discriminate in the orientational effects *vis-à-vis* non-bonded interactions between these ligands and various residues at the active site.

Docking studies

FlexiDock. Plate 2 is a scatter plot of observed biological activity and calculated docking scores with both COX-1 and COX-2. Docking results of all diaryloxazolones with COX-2 show some correlation with biological activity; molecules with better activity fitted better. Similarly, docking of various oxazolones into the COX-1 active site also showed a variable correlation between the observed inhibitory activities and fitness scores. However, almost all ligand molecules produced less favourable scores (high energy) compared with the corresponding complexes with COX-2. These observations correspond with biological activities towards COX-1, i.e. all these molecules are relatively weak inhibitors of COX-1.

Docking of the COX-2 selective inhibitors like celecoxib and rofecoxib into the active sites of both forms of cyclooxygenase produced scores, that are in agreement with the observed activities (Plate 2). The orientations of oxazolone **29** (Plate 3b) and rofecoxib (**III**) in COX-2 are very similar and are shown in plate 3a. All other oxazolones are also found with similar orientations, but they assume different orientations in COX-1.

Affinity. Docking studies with COX-2 using Affinity were carried out on three diaryloxazolones, **18, 25** and **29** (differing in inhibition levels), and two COX-2 - selective inhibitors, *viz*. celecoxib and rofecoxib. Docking of each ligand into the COX-2 active site generated a number of possible structures with different orientations of ligand

Table 3. Interaction energies (kcal mol^{-1}) between celecoxib, rofecoxib, oxazalones **29, 18** and **25** and various amino acid residues of the COX-2 active site

Residue	Celecoxib[a]	Rofecoxib[b]	**29**[c]	**18**[d]	**25**[e]
His 90	−2.19	−1.53	−1.87	−0.82	−0.50
Val 116	−0.60	–	−0.25	−0.16	−0.35
Arg 120	−0.66	0.12	1.60	−2.03	−1.25
Gln 192	−0.73	0.72	1.13	−0.28	–
Tyr 348	−0.47	−0.59	−2.56	−0.03	−0.62
Val 349	−1.85	−1.90	−3.82	−1.23	−1.87
His 351	−0.97	–	−3.27	–	–
Leu 352	−5.11	−0.27	−6.50	−2.23	−1.52
Ser 353	0.97	−0.58	−1.57	−1.61	−1.20
Gly 354	0.11	−0.61	0.99	−0.19	–
Tyr 355	−1.57	−2.20	−4.30	−3.01	−0.53
Leu 359	−0.58	−0.13	0.75	−0.39	−0.27
Phe 381	−0.17	−0.29	−1.00	0.04	−0.14
Leu 384	−0.14	−0.30	−0.58	−0.03	−0.21
Tyr 385	−0.58	−0.93	−1.58	−0.93	−0.06
Trp 387	−0.39	−0.38	0.42	−1.23	−0.52
Arg 513	−1.63	0.81	−0.07	−0.35	−2.34
Ala 516	0.07	−1.31	0.18	0.01	–
Ile 517	0.03	−2.28	0.36	−0.08	0.02
Phe 518	−2.23	−4.01	−0.95	−1.12	−0.21
Met 522	−0.42	−0.80	−3.52	−4.973	−0.70
Val 523	−1.85	−0.93	−3.64	−2.73	−2.66
Glu 524	–	–	−1.70	−0.33	−3.68
Gly 526	−1.12	0.48	1.37	0.81	−0.08
Ala 527	−1.83	−0.01	0.09	−0.95	−0.25
Phe 529	−0.26	–	–	–	–
Ser 530	−0.39	−4.45	−0.21	−1.13	−2.31
Leu 531	−0.44	−1.03	0.10	−0.75	−1.02
Energy	−29.61	−26.06	−29.80	−26.12	−24.01
Activity (IC_{50})	0.04	0.02	0.23	0.79	18.9

[a] Residues Thr 94 (−0.31) Met 113 (−0.4), Leu 117 (−0.17), Phe 357 (−0.19), Gly 519 (0.45) and Pro 528 (−0.44) also interact with celecoxib and their non-bonded energies are given in the parentheses.
[b] Gly 519 (−0.82).
[c] Thr 94 (0.59).
[d] Thr 521 (−0.64), Leu 525 (0.21).
[e] Pro 86 (−0.07), Val 89 (−0.48), Leu 93 (0.40), Ile 345 (−0.09).

inside the active site, each with different energy. The most energetically favourable conformation for each ligand in the COX-2 complex was chosen for further analysis. Non-bonded interaction energies between ligand and various amino acid residues at the active site are given in Table 3. The orientations of all five ligands in COX-2 are very similar, even though the hydrogen bonding and other non-bonded interaction patterns differ slightly.

The orientation and hydrogen bonding interactions of celecoxib (**I**), in COX-2 is shown in Plate 4. The orientation of **I** is very similar to that of SC-558 (**III**).[21,30] However, different sets of hydrogen bonding interactions with residues His 90, (N—H···O=S 1.88 Å) and Phe 518 (N—H···O=S 3.04 Å) are observed.[30] In the case of rofecoxib the hydrogen bonding interactions are observed with residues Gln 192 (N—H···O=S 2.84 Å), Phe 518 (N—H···O=S 2.12 Å) and Ser 530 (O—H···O=C 2.06 Å) (Plate 5). In the case of nimesulide,[31,32] no significant hydrogen bonding interactions are observed with any these residues. The orientation and hydrogen bonds formed by the most active oxazolone, **29**, are shown in Plate 6. The orientation is nearly similar to that of SC-558 and celecoxib. Very strong hydrogen bonds are found with residues His 90 (N—H···O=S 1.79 Å), Ser 353 (C=O···H—N 1.73 Å) and Leu 352 (C=O···H—N 1.80 Å). Molecule **18** is moderately active and is bound in a similar orientation. The hydrogen bonds with Leu 352 (C=O···H—N 1.76 Å), Ser 353 (C=O···H—N 1.71 Å), Arg 513 (N—H···O=S 2.31 Å) and Ser 530 (O—H···O=C 1.75 Å) differ significantly from **29**.[33] The less active **25** is also bound in a similar orientation, but moves towards the entrance of the active site cleft, contributing to the differences in steric and electrostatic interactions. The hydrogen bonds of **25** with His 90 (N—H···O=S 2.39 Å), Gln 192 (C=O···H—N 1.89 Å) and Leu 352 (C=O···H—N 1.73 Å) are different from **29** and **18**. In general, the other non-bonded interactions also follow similar trends (Table 3).

The steric interaction energies of celecoxib, rofecoxib and oxazolones **29, 18** and **25** with various amino acid

residues in the active site are plotted in Plate 7a and the electrostatic contributions are given in Plate 7b. In general, celecoxib, rofecoxib and oxazolones **29, 18** and **25** optimize similar types of interaction with various amino acid residues in the active site, but molecule **25** is involved in less favourable interactions (Fig. 4a) with the hydrophobic cleft that extends towards the peroxide catalytic site. This difference contributes to the lower activity of molecule **25**. The steric interactions of the highly selective inhibitor rofecoxib with various residues at the 'mouth' of the active site are similar to celecoxib (Plate 7a). As for the electrostatic interaction energy contributions, celecoxib, rofecoxib and molecule **29** show a similar pattern nearly everywhere in the active site (Plate 7b). However, oxazolones **25** and **18** differ widely in some regions. Affinity calculations of these ligands with COX-1 produce highly repulsive contacts and the energies produced are definitely unacceptable.

CONCLUSIONS

3D-QSAR–CoMFA and docking studies have been performed on a novel series of 3,4-diaryloxazolones that are reported to be specific COX-2 inhibitors. The final model is reasonably good and its predictive reliability has been validated by a set of test molecules. Correlations were made between biological activity and steric and electrostatic fields. Subsequently, all the ligands were docked in the active sites of both COX-1 and COX-2. A good correlation between the docking score and biological activity was obtained for all compounds studied. Detailed interaction energy calculations, subsequent to docking of a group of known and putative COX-2-selective molecules with the active site residues, extend this correlation qualitatively.[34,35] From this study it is clear that COX-2 selectivity can be achieved by structure-based drug-design approaches and that 3,4-diaryloxazolones are good candidates for the purpose.

Acknowledgements

We thank Professor R. Kumar for helpful discussions. CSIR is thanked for financial support in the form of project 90/008/99/EMR-II. RT thanks CSIR for a senior research fellowship under the project 37(999)98-EMR-II and DR thanks UGC for a senior research fellowship.

REFERENCES

1. Hia T, Nielson K. *Proc. Natl. Acad. Sci. U. S. A.* 1992; **89**: 7384–7388.
2. Jones DA, Carlton DP, McIntyre TM, Zimmerman GA, Prescott SM. *J. Biol. Chem.* 1993; **268**: 9049–9054.
3. Kennedy B, Chan CC, Culp S, Cromlish W. *Biochem. Biophys. Res. Commun.* 1993; **197**: 494–500.
4. Kujubu DA, Fletcher BS, Varnum BC, Lim RW, Herschman H. *J. Biol. Chem.* 1991; **266**: 12866–12872.
5. Chipman JG, Erikson RL. *Proc. Natl. Acad. Sci. U.S.A.* 1997; **88**: 2692–2696.
6. Needleman P, Isakson PC. *Rheumatology* 1997; **24**: 6–8.
7. Vane JR, Botting RM. *Inflamm. Res.* 1998; **47**: S78–S87.
8. Katori M, Majima M, Harada Y. *Inflamm. Res.* 1998; **47**: S107–S111.
9. Sawdy R, Slater D, Fisk N, Edmonds DK, Bennet P. *Lancet* 1997; **350**: 265–266.
10. Kutchera W, Jones DA, Matsunami N, Groden J, McIntyre TM, Zimmerman GA, White RL, Prescott SM. *Proc. Natl. Acad. Sci. U. S. A.* 1996; **93**: 4816–4820.
11. Stewart WF, Kawas C, Corrada M, Metter EJ. *Neurology* 1997; **48**: 626–632.
12. Li CS, Black WC, Brideau C, Chan CC, Charleson S, Cromlish WA, Claveau D, Gauthier JY, Gordon R, Greig G, Grimm E, Guay J, Lau CK, Riendeau D, Therein M, Visco DM, Wong E, Xu L, Prasit P. *Bioorg. Med. Chem. Lett.* 1999; **22**: 3181–3186.
13. Dube D, Brideau C, Deschenes D, Fortin R, Friesen RW, Gordon R, Girard Y, Riendeau D, Savoie C, Chan CC. *Bioorg. Med. Chem. Lett.* 1999; **12**: 1715–1720.
14. Lazer ES, Sorcek R, Cywin CL, Thome D, Possanza GJ, Graham AG, Churchill L. *Bioorg. Med. Chem. Lett.* 1998; **10**: 1181–1186.
15. Bayly CI, Black WC, Leger S, Ouimet N, Ouellet M, Percival MD. *Bioorg. Med. Chem. Lett.* 1999; **3**: 307–312.
16. Khanna IK, Yu Y, Huff RM, Weier RM, Xu X, Koszyk FJ, Collins PW, Cogburn JN, Isakson PC, Koboldt CM, Masferrer JL, Perkins WE, Seibert K, Veenhuizen AW, Yuan J, Yang DC, Zhang YY. *J. Med. Chem.* 2000; **43**: 3168–3185.
17. Churchill L, Graham A, Shih CK, Pauletti D, Farina PR, Grob PM. *Inflammopharmacology* 1996; **4**: 125–135.
18. Glaser K, Sung ML, O'Neill K, Belfart M, Hartman D, Carlson R, Kreft A, Kubrak D, Hsiao CL, Weichman B. *Eur. J. Pharmacol.* 1995; **281**: 107–111.
19. Simon LS, Lanza FL, Lipsky PE, Hubbard RC, Talwalker S, Schwartz BD, Isakson PC, Geis GS. *Arthritis Rheum*. 1998; **41**: 1591–1602.
20. Lloyd AW. *Drug Discovery Today* 2000; **5**(3): 121–122.
21. Kurumbail RG, Stevens AM, Gierse JK, McDonald JJ, Stegeman RA, Pak JY, Gildehaus D, Miyashiro JM, Penning TD, Seibert K, Isakson PC, Stallings WC. *Nature* 1996; **384**: 644–648.
22. Talley JJ, Brown DL, Carter JS, Graneto MJ, Koboldt CM, Masferrer JL, Perkins WE, Rogers RS, Shaffer AF, Zhang YY, Zweifel BS, Seibert K. *J. Med. Chem.* 2000; **43**: 775–777.
23. Desiraju GR, Gopalakrishnan B, Jetti RKR, Raveendra D, Sarma JARP, Subramanya HS. *Molecules* 2000; **5**: 945–955.
24. Puig C, Crespo MI, Godessart N, Fexias J, Ibarzo J, Jimenez J, Soca L, Cardelus I, Heredia A, Miralpeix M, Puig J, Beleta J, Huerta JM, Lopez M, Segarra V, Ryder H, Palacious JM. *J. Med. Chem.* 2000; **43**: 214–223.
25. SYBYL 6.6 Molecular Modelling Software, Tripos Associates Inc., 1699 S Hanley Rd., St. Louis, MO 631444, USA.
26. Abola EE, Berstein FC, Bryant SH, Koetzle TF, Weng J. Protein Data Bank. In *Crystallographic Databases — Information Content, Software Systems, Scientific Applications*, Allen FH, Berjerhoff G, Sievers R (eds). Data Commission of the International Union of Crystallography: Bonn, 1987; 171.
27. Clark M, Cramer III RD, Jones DM, Patterson DE, Simeroth PE. *Tetrahedron Comput. Method.* 1990; **3**: 47–59.
28. Insight II, Release 97.0; Molecular Simulations Inc.: San Diego, CA, 1997.
29. Loll PJ, Picot D, Ekabo O, Garavito RM. *Biochemistry* 1996; **35**: 7330–7340.
30. Price MLP, Jorgensen WL. *J. Am. Chem. Soc.* 2000; **122**: 9455–9466.
31. Fabiola GF, Pattabhi V, Kuppuswamy N. *Bioorg. Med. Chem.* 1998; **6**: 2337–2344.
32. Garcia-Nieto R, Perez C, Gago F. *J. Comput. Aided Mol. Des.* 2000; **14**: 147–160.
33. Oriol L, Juan JP, Albert P, David M. *Bioorg. Med. Chem. Lett.* 1999; **9**: 2779–2784.
34. Vieth M, Cummins DJ. *J. Med. Chem.* 2000; **43**: 3020–3032.
35. Kastenholz MA, Pastor M, Cruciani G, Haaksma EEJ, Fox T. *J. Med. Chem.* 2000; **43**: 3033–3044.